

---

# A Simple Method to Reduce Off-chip Memory Accesses on Convolutional Neural Networks

---

Anonymous Authors<sup>1</sup>

## Abstract

For convolutional neural networks, a simple algorithm to reduce off-chip memory accesses is proposed by maximally utilizing on-chip memory in a neural process unit. Especially, the algorithm provides an effective way to process a module which consists of multiple branches and a merge layer. For Inception-V3 on Samsung’s NPU in Exynos, our evaluation shows that the proposed algorithm makes off-chip memory accesses reduced by 1/50, and accordingly achieves 97.59% reduction in the amount of feature-map data to be transferred from/to off-chip memory.

## 1. Introduction

Recent achievements in image processing tasks such as image recognition, object detection, and scene segmentation have been coupled with the application of deep convolutional networks (Szegedy et al., 2015; Ren et al., 2015; Long et al., 2015). As the need for more complex networks increases, we get faced with several implementation issues, i.e. real time processing, limited power budget, and memory bandwidth. For the issues to get resolved, various approaches have been investigated in both cloud and mobile applications; low-precision (Courbariaux et al., 2014; 2015; Hubara et al., 2016; Gupta et al., 2015; Gysel et al., 2016; Judd et al., 2015; Lin et al., 2016; Kim et al., 2018), network compression (Han et al., 2015), (Han et al., 2016b), and small network design (Iandola et al., 2016), (Howard et al., 2017).

Another remarkable trend is to execute deep convolutional networks on mobile platforms, and it is getting important by concerns about response time, dependency on an internet connection, privacy, and security. Many companies and research groups have been recently developing notable hardware accelerators called as a neural processing unit (NPU)

(Song et al.; Zhang et al., 2016; ARM-ML-processor). They tried to develop energy-efficient NPUs based on novel algorithms such as exploiting network sparsity for high utilization of multiply/accumulate (MAC) units or quantizing networks to reduce the power of MAC units. To operate CNNs on a NPU, it is needed to access memory hugely to read and write weight and feature-map data. In (Han et al., 2016a), it was shown that the total energy is dominated by the required memory access if there is no data reuse, and that the energy cost of on-chip memory (SRAM in (Han et al., 2016a)) is 128 times better than one of off-chip memory (DRAM in (Han et al., 2016a)). Since NPUs for a mobile platform have the limited amount of on-chip memory, however, it is not easy to maintain NPU efficiency for most applications. Therefore, we reasoned that reducing off-chip memory accesses by utilizing on-chip memory maximally can be one of the most powerful solutions to increase the efficiency of NPUs.

To achieve the high utilization of on-chip memory, we needed to know what series of operations are required in NPUs for processing the convolution layer and to choose the most efficient one among possible series of operations. We focused on a series of operations which fetches weights in minimal increments and executes convolution with the weights for the feature-maps of all input channels. Such a series of operations makes the realization of convolution simple by leaving out the consideration about how to locate weights in on-chip memory. Figure 1 shows the required memory size of weights and feature-maps according to the index of layer, for Inception-V3 and ResNet-50. The size of weights increases as the layer index increases, whereas the size of feature-maps decreases as the layer index increases. From the patterns of sizes, we thought that it would be beneficial to locate feature-maps fully in on-chip memory and to manage them efficiently if the size of feature-maps is small enough to be located in on-chip memory. In recent architectures of convolutional neural networks, moreover, a concept of module or block has been introduced to computer vision applications for higher representational power of neural networks. The important thing of such observation is that modules or blocks are repeatedly used in a network just after feature-maps are scaled down for reduction of computational cost, as shown in Figure 1. Depending on

---

<sup>1</sup>Anonymous Institution, Anonymous City, Anonymous Region, Anonymous Country. Correspondence to: Anonymous Author <anon.email@domain.com>.

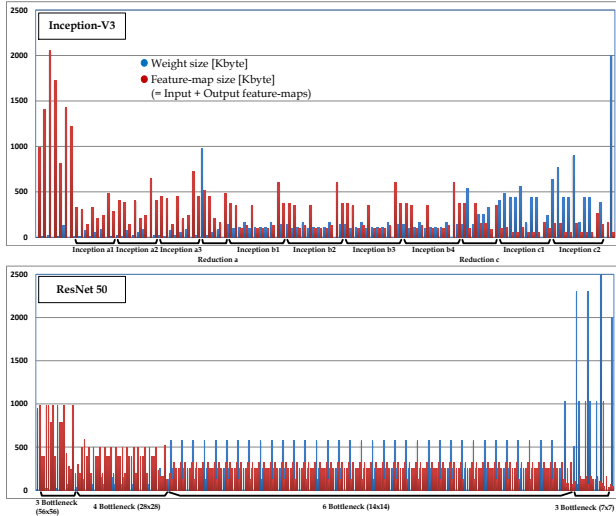


Figure 1. Sizes of weights and feature-maps according to indexes of layers for Inception-V3 and ResNet-50.

the size of feature-maps and the characteristics of modules, therefore, we were able to find a simple way to minimize off-chip memory accesses by efficiently managing on-chip memory for modules.

In this paper, we propose a simple method to support energy-efficient and real-time processing of NPUs through the reduction of off-chip memory accesses. Firstly, the algorithm detects certain types of modules or blocks by graph interpretation of the whole network. Then, several regions of on-chip memory are assigned to reuse feature-maps during a module or a block processing. In order to utilize on-chip memory maximally, moreover, we also propose a branch-reordering algorithm and two branch-processing algorithms. By combining the proposed algorithms, we can effectively cut down off-chip memory accesses for convolutional neural networks such as Inception-V3 and ResNet. The rest of the paper is organized as follows. Section 2 describes the module we define. Then, in Section 3, we introduce the proposed algorithms to reduce off-chip memory accesses. Section 4 shows evaluation results for a representative network, Inception-V3 (Szegedy et al., 2015; 2016). Finally, Section 5 makes a conclusion.

## 2. Definition of Module

After Network-in-Network was proposed in (Lin et al., 2013) in order to increase the representational power of neural networks, a concept of module or block is getting popular in convolution neural networks for computer vision applications like Inception network (Szegedy et al., 2015; 2016), ResNet (He et al., 2016), MobileNet V2 (Sandler et al., 2018), SqueezeNet (Iandola et al., 2016), ShuffleNet (Ma

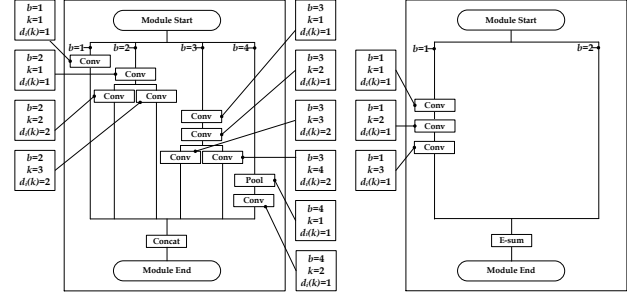


Figure 2. Illustration of various modules satisfying four conditions in Section 2. Here,  $b$  and  $k$  denote the indexes of a branch and a layer for the module, And  $d_i(k)$  is the maximum depth of module at the  $k^{th}$  layer.

et al., 2018), and MnasNet (Tan et al., 2018). In this section, we define module and specify which modules can be utilized in the algorithms we will propose among the modules defined for various networks.

In general, a module used in convolutional neural networks can be one of the directed acyclic graphs (DAGs), which is a finite directed graph without directed cycles. That is, it consists of finite multiple layers and edges, with each edge directed from one layer to another, such that there is no way to start at any layer  $A$  and follow a consistently-directed sequence of edges that eventually loops back to  $A$  again. For a convolutional neural network including many modules, moreover, it can be viewed as a large DAG with multiple DAGs.

In the paper, we consider only the limited structure of DAGs satisfying the following conditions: 1) the module has multiple branches within itself, 2) the module has to include at least a merge layer, and 3) the type of merge layers should be either concatenation or element-wise summation. In addition, 4) we do not cover a large-sized module configured by a long skip-connection or having lots of layers inside, which has been frequently used in neural networks to extract multi-scaled features. This is because there seems no efficient way to utilize on-chip memory for large-sized modules. When we focused on only the modules satisfying the four conditions mentioned above, we could reach a sub-optimal but simple solution to reduce off-chip memory accesses even if the proposed algorithms did not cover all kinds of neural networks.

Figure 2 shows the examples of modules satisfying the required conditions and introduces some useful indices to explain the algorithms proposed in this paper, where  $b$  denotes the index of branch in a module,  $k$  is the index of layer in a branch, and  $d_i(k)$  denotes the maximum depth of modules for the  $k^{th}$  layer. In other words, it means  $k^{th}$  layer is included in the  $d_i(k)^{th}$  module. With these parameters,

we explain two types of modules, each having a different kind of merge layer as follows:

**Concatenation based module:** this type of module includes the  $k$ -th layer on the  $b$ -th branch, and a concatenation layer at the end of module, as shown in the left plot of Figure 2. Sometimes the module also includes the sub-module which is a module in a module like as the Inception-C type. The representative neural networks having the concatenation based module are several versions of Inception Networks (Szegedy et al., 2015; 2016) and SqueezeNet (Iandola et al., 2016). In Figure 2, *Conv* and *Pool* mean a convolutional layer and a pooling layer, respectively.

**Element-wise adder based module:** this type of module has two branches, multiple layers, and an element-wise adder at the end. The representative neural networks with the element-wise adder based module are ResNet (He et al., 2016) and MobileNet V2 (Sandler et al., 2018).

### 3. Algorithm for Effective Module Processing

The flowchart demonstrated in Figure 3 shows an overall process of compiler optimization including the algorithm proposed for module processing, where the compiler serves to interpret graphs as well as to make a policy for effective execution of a neural network on NPUs. *Neural network source code* represents a certain type of files including graph information of a neural network such as prototxt and TFLite formats. Through *parse unit*, network parameters are extracted such as kernel size, stride, pad, layer type, feature-map size, module parameters and so on. With the extracted parameters, we can operate the proposed algorithm in *optimization unit* which includes four phases: *module detection*, *micro-instruction generation*, *branch reordering* and *branch processing (I/II)*. Here, *module detection* is to detect the modules satisfying required conditions in a neural network, and *micro-instruction generation* is to find the best sequence of micro-instructions per module defined in NPU. *branch reordering* decides on a new order of branches to be processed in a module based on a proposed criteria. And *branch processing I/II* decide an effective policy. Then, *memory allocation unit* executes a resource allocation of on-chip memory based on the policy by the optimization unit. Finally, *neural network object code* is generated as an output of *object code generation unit*.

Since our main proposal is *optimization unit* in Figure 3, we explain it in detail. Algorithm 1 shows a whole procedure of *optimization unit* which has six steps such as module detection, operator sequence generation, branch reordering, MIFM (Module’s Input Feature Map) memory size calculation, occupied MOFM (Module’s Output Feature Map) memory size calculation, and branch processing. Here, a network graph  $\Omega$  is used as an input in *optimization unit*,

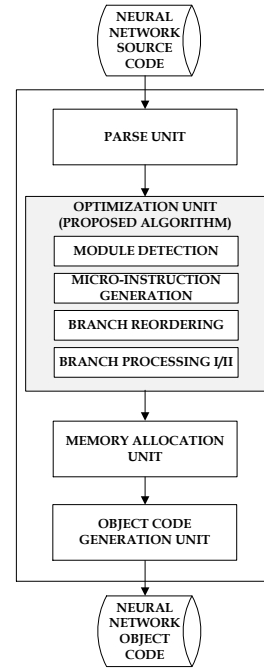


Figure 3. Overall flowchart of the compiler optimization including the proposed algorithm.

and there are two types of outputs: the best sequence of micro-instructions, and the resource allocation information in on-chip memory per module. Each step of Algorithm 1 is described in detail in Algorithm 2 through Algorithm 6.

First of all, the proposed algorithm has to detect all possible valid modules within a network. Different kinds of modules are designed for well-known neural network models, but we focus only on those modules which are suitable for efficient use of on-chip memory. Algorithm 2 is about how to detect modules that meet the required conditions as mentioned in the previous section. First, we skip modules configured by a long skip-connection since it is extremely difficult to manage them within on-chip memory efficiently. Then, the algorithm detects modules in a modified graph where all the long skip-connections are erased.

Figure 4 shows the results of the module detection algorithm being applied to Inception-V3. Here we can see that 11 modules are detected by the Algorithm 2. After detecting modules, the optimization unit generates a sequence of micro-instructions for whole layers of each module. Since this step is very hardware-dependent, it is hard to explain details in this paper. In the optimization unit, anyway, the best sequence of micro-instructions should be found in order to make the layers of each module processed efficiently in a specific hardware.

As the 3<sup>rd</sup> step, we execute a re-ordering process of



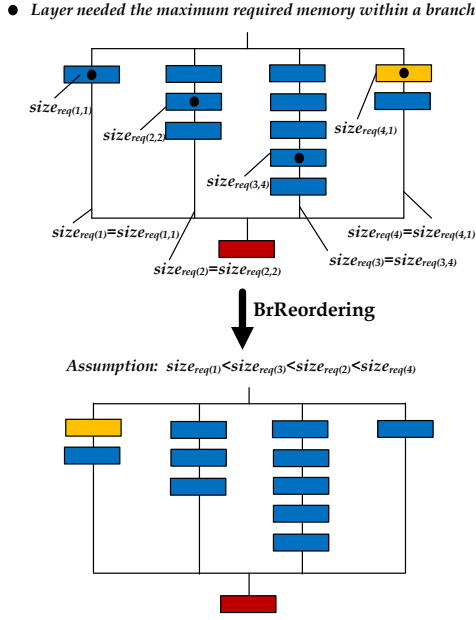


Figure 5. Illustration of the branch re-ordering algorithm in Algorithm 3

in Algorithm 4, sizes and offsets are calculated at the  $k^{th}$  layer for all possible depths,  $d_i(k)$ , in the module. In Figure 6, we look at the red-colored box as an example of MIFM calculation algorithm, where it is the second branch with three layers in the module. If you look at the 1<sup>st</sup> layer, only  $size_{mifm(1,1)}$  is considered because it is included in the only 1<sup>st</sup> depth module. Because  $size_{mifm(1,1)}$  is exactly same with the size of the previous branch, of course, the memory region is directly handed over from the previous branch. For the 2<sup>nd</sup> and the 3<sup>rd</sup> layers within the 2<sup>nd</sup> depth module, we need to consider the second shared memory region of  $size_{mifm(2,2)}$  and  $offset_{mifm(2,2)}$ . After operating the 3<sup>rd</sup> layer, we can release the second shared memory region of  $size_{mifm(2,2)}$  and  $offset_{mifm(2,2)}$  because there is no need in the next branches.

**Algorithm 4** Calculation of MIFM size for the  $k^{th}$  layer,  $CalSizeMifmMem(k)$

**Input:** module parameters  $\omega$ , effective depth of MIFM for the  $k^{th}$  layer in module  $d_i(k)$ .

**for**  $i = 1$  to  $d_i(k)$  **do**

    % calculating MIFM size for the module with  $\omega$

$size_{mifm(k,i)} = calcMifmMemSize(k, i)$

$offset_{mifm(k,i)} = calcMifmMemOffset(k, i)$

**end for**

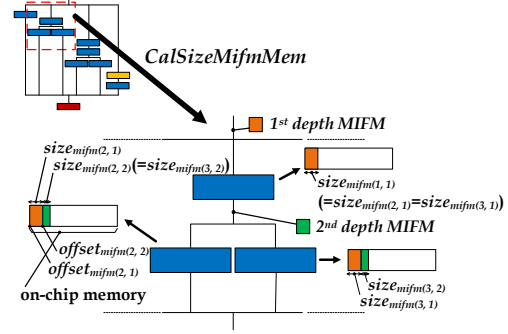


Figure 6. Illustration of the MIFM calculation algorithm in Algorithm 4

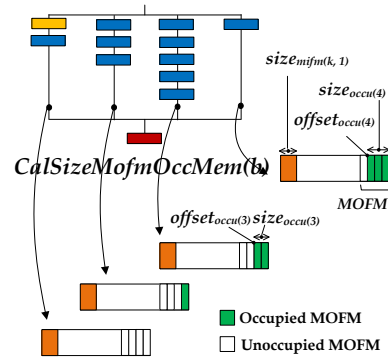


Figure 7. Illustration of the occupied MOFM calculation algorithm in Algorithm 5

As the 5<sup>th</sup> step, we calculate the occupied memory sizes within MOFM at the  $b^{th}$  branch in Algorithm 5. It can be simply calculated by accumulating the output size of the last layer on all previous branches. It means  $size_{occu(b)}$  is the size of occupied region of the MOFM for the current branch as shown in Figure 7. It is important to exactly calculate the size of the occupied region because the region (green colored region in Figure 7) in on-chip memory cannot be utilized for the current branch operations.

The branch processing is conducted at the last step as shown

**Algorithm 5** Calculation of the occupied memory size of MOFM at the  $b^{th}$  branch,  $CalSizeMofmOccMem(b)$

**Input:** module parameters  $\omega$ .

$size_{occu(b)} = 0$

**for**  $i = 1$  to  $b - 1$  **do**

$size_{occu(b)} += calcMofmMemSize(i)$

$offset_{occu(b)} = calcMofmMemOffset(i)$

**end for**

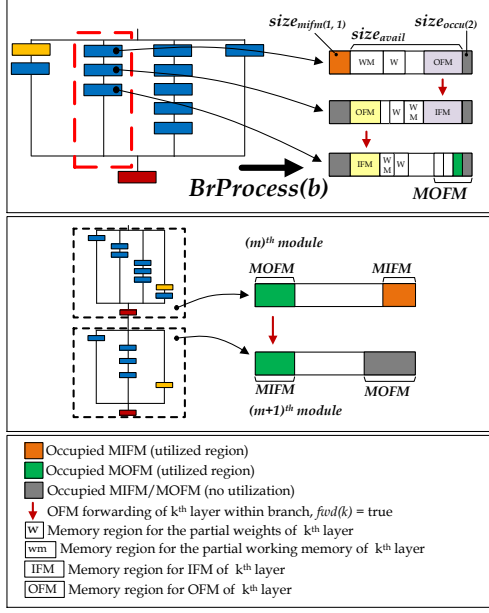


Figure 8. Illustration of the branch processing algorithm in Algorithm 6

in Algorithm 6. We propose two types of branch processing: (I) default algorithm considering both MIFM and MOFM, and (II) optional algorithm considering only MIFM. The optimization unit adaptively chooses one between (I) and (II) according to the required memory size of a module. The branch processing (I) can support an operation where MOFM of the former module is directly forwarded to MIFM of the latter module (= sharing memory between consecutive modules), but we have to use less memory region ( $size_{avail}$  in Figure 8) within branch operation because it needs the occupied memory region for both MIFM and MOFM in the module. In other hands, the branch processing (II) is an optional algorithm applicable when a required memory size  $size_{req}(b)$  for the  $b^{th}$  branch is larger than that of available on-chip memory  $size_{avail}(b,k)$ . It is because we can use additional memory region of  $size_{occu}(b)$  for a branch processing and because we can also get more available memory by considering  $size_{OFM.Partial}$ , not  $size_{OFM.Full}$  at the last layer on the branch. That is, we give up the shared memory region of MOFM in order to increase  $size_{avail}$ , instead we get a benefit only from sharing MIFM on the branch. More detail operations are explained in Algorithm 6, where  $fwd(k)$  denotes a flag of an OFM forwarding of the  $k^{th}$  layer. Figure 8 shows the example of the branch processing (I), where we consider the second branch operation including three layers within a module. At the 1<sup>st</sup> layer,  $size_{mifm(1,1)}$  means the shared memory for MIFM in the module, and  $size_{occu(2)}$  is mapped to the occupied region by OFM of last layer in the 1<sup>st</sup> branch. That is, we

#### Algorithm 6 Branch processing, $BrProcess(b, opt)$

**Input:** Branch index  $b$ , and MIFM depth  $d_i(k)$ , and pre-occupied MOFM size  $size_{occu}(b)$

```

 $fwd_{(0)} = \text{false};$ 
% estimating the forwarding status of OFM for the  $k^{th}$ 
layer on the branch
for  $k = 1$  to  $len(\text{layers of branch})$  do
% calculating the available memory size
if  $opt = 'II'$  then
 $size_{occu}(b) = 0$ 
end if
 $size_{avail}(b,k) = size_{mem} - \sum_{m=1}^{d_i(k)} size_{mifm}(k,m) -$ 
 $size_{occu}(b)$ 
if ( $fwd_{(k-1)}$ ): then
 $size_{req}(b,k) = size_{IFM.Full} + size_{OFM.Full} +$ 
 $size_{WM.Partial} + size_{W.Partial}$ 
if  $size_{req}(b,k) \leq size_{avail}(b,k)$ : then
 $fwd_{(k)} = \text{true};$ 
else
 $fwd_{(k)} = \text{false};$ 
end if
else
 $size_{req}(b,k) = size_{IFM.Partial} + size_{OFM.Full} +$ 
 $size_{WM.Partial} + size_{W.Partial}$ 
if  $size_{req}(b,k) \leq size_{avail}(b,k)$ : then
 $fwd_{(k)} = \text{true};$ 
else
 $fwd_{(k)} = \text{false};$ 
end if
end if
if ( $opt = 'II'$ ) and ( $k == len(\text{layers of branch})$ ) then
 $fwd_{(k)} = \text{false};$ 
%  $size_{req}(b,k)$  can be calculated with
 $size_{OFM.Partial}$ , not  $size_{OFM.Full}$ .
end if
end for
    
```

can use only  $size_{avail}$  which is defined in Figure 8 for the 1<sup>st</sup> layer. If the total size including OFM, working memory (WM) and weights (W) is equal to or less than  $size_{avail}$ , OFM can be directly forwarded to IFM of the 2<sup>nd</sup> layer, as shown in Figure 8. At the 3<sup>rd</sup> layer by the same sequences, IFM is a heritage region from OFM of the second layer and OFM is stored as the green colored region within MOFM region. By using the branch processing (I), therefore, we can completely erase off-chip memory accesses during the processing within a module. The algorithm also provides the removal of the off-chip accesses between consecutive modules by forwarding the MOFM of the former module to the MIFM of the latter module in neural networks, as shown in the second plot of Figure 8.

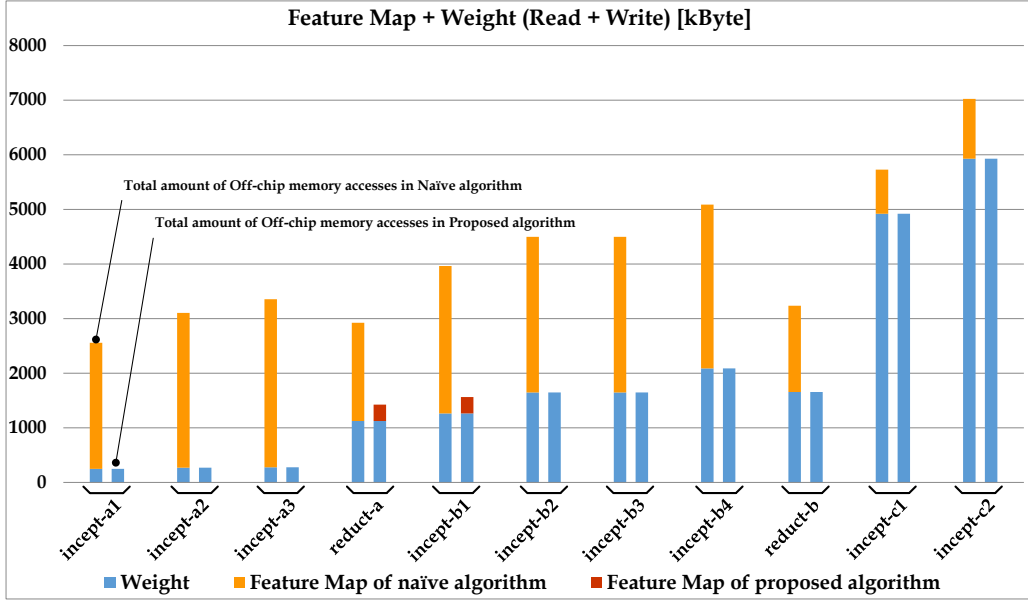


Figure 9. Comparison of total data sizes accessed the off-chip memory for Naive and Proposed algorithms, where total data size was summed for both weights and feature-maps.

#### 4. Evaluation

To evaluate the proposed algorithm, a representative CNN model, Inception-V3 (Szegedy et al., 2016) with an input image of  $299 \times 299$ , has been selected. The target neural processor and its features are as follows: 1) Samsungs NPU (Song et al.) in Exynos has 1024 multiply/accumulate (MAC) units on 16 MAAs (multiply/accumulate arrays), and on-chip memory of 1,024 Kbyte which contains IFMs, OFMs, weights and temporary WMs. The NPU also has 3 parallelism: First, IFMs are divided and fetched into four chunks along channel. Second, OFMs in the form of  $4 \times 4$  patch in a MAA are computed in parallel. Lastly, a weight kernel is copied to 16 kernels for parallel operation on 16 MAAs. 2) It is not essential that all weight kernels of a layer have to be in on-chip memory. The NPU can make 16 OFM channels in parallel if partial weights for 16 MAAs are in on-chip memory. The partial weights can be read and written in a double buffering manner to effectively hide memory access time. 3) We assume that all weights and feature-maps are 8-bit quantized in the evaluation, even though the NPU supports other precisions.

Figure 9 shows the total amount of data with off-chip memory access for two algorithms: Naive and Proposed algorithms. Here, it is assumed that Naive algorithm has to access off-chip memory to read and write feature-maps for every layers. The results show that the amount of feature-map with off-chip memory access is almost gone and the amount of weight with off-chip memory access remains the same. Therefore, the proposed algorithm reduces the total

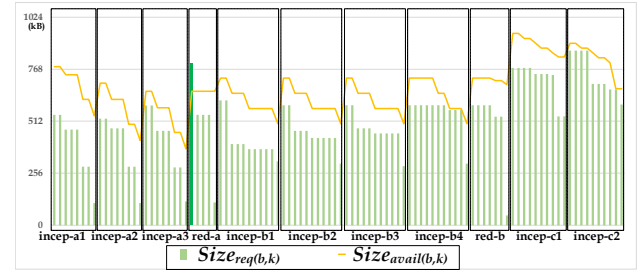


Figure 10. Illustration of the relationship between  $size_{req}(b,k)$  and  $size_{avail}(b,k)$  through the proposed algorithm at the  $k^{th}$  layer on the  $b^{th}$  branch for 11 modules in Inception-V3.

amount of data with off-chip memory access by almost half. By applying the proposed algorithm, only *reduction-a* and *Inception-b1* among 11 modules in Inception-V3 have a little amount of feature-map with off-chip memory access. The reason can be explained as follows: In *reduction-a* module, we operated  $BrProcessing(b, II)$  which needs to access off-chip memory three times at the end of branches because  $size_{req}$  was not satisfied with  $size_{avail}$  for the module, as shown in Figure 10. That is why the off-chip accesses in *reduction-a* happen. And then, there exists one time of off-chip memory access at the start of the *Inception-b1* module according to the result of the former module, *reduction-a*. Figure 10 shows the important information related to  $size_{req}(b,k)$  and  $size_{avail}(b,k)$  in our proposed algorithm. Firstly, branches in each module are re-ordered by  $size_{req}(b,k)$ . And  $size_{avail}(b,k)$  also decreases as the in-

	Amount of off-chip memory accesses [KB]							(For FM) Number of off-chip memory accesses			
	W	Naive		Proposed		Overall Ratio [%]	FM Ratio [%]	Naive		Proposed	
		FM	Overall	FM	Overall			Read	Write	Read	Write
inception-a1	249	2308.5	2557.5	0	249	9.74	0.00	8	8	0	0
inception-a2	270	2835	3105	0	270	8.70	0.00	8	8	0	0
inception-a3	277.5	3078	3355.5	0	277.5	8.27	0.00	8	8	0	0
reduction-a	1125	1798.5	2923.5	300	1425	48.74	16.68	5	5	0	3
inception-b1	1264	2700	3964	300	1564	39.46	11.11	11	11	1	0
inception-b2	1648	2850	4498	0	1648	36.64	0.00	11	11	0	0
inception-b3	1648	2850	4498	0	1648	36.64	0.00	11	11	0	0
inception-b4	2088	3000	5088	0	2088	41.04	0.00	11	11	0	0
reduction-b	1656	1580	3236	0	1656	51.17	0.00	7	7	0	0
inception-c1	4920	808	5728	0	4920	85.89	0.00	10	10	0	0
inception-c2	5928	1096	7024	0	5928	84.40	0.00	10	10	0	0
total	21073.5	24904	45977.5	600	21673.5	47.14	2.41	100	100	1	3

Table 1. Summary about the amount and the number of the off-chip accesses for 11 modules in Inception-V3, where FM and W mean a feature-map and a weight, respectively.

dex of branch in the module increases because  $size_{occu(b)}$  increases. Moreover, we can see the relationship between  $size_{req(b,k)}$  and  $size_{avail(b,k)}$  used for the criteria to select  $BrProcessing(b, I)$  or  $BrProcessing(b, II)$ .

Consequently, Table 1 summarizes the overall amount of off-chip accesses for every modules in Inception-V3, and an reduction ratio is calculated to 47.14 % (=21673.5 / 45977.5). And The table also represents the amount and the number of off-chip accesses for only a feature-map in Inception-V3. We can know that the proposed algorithm can achieve a great reduction up to 97.59 % in terms of the amount, and can effectively reduce to 1/50 (= 4/200) in terms of the number of accesses for all modules.

## 5. Conclusion

In the paper, we proposed a simple method for energy-efficient and real-time processing of NPUs through the reduction of off-chip memory accesses. To achieve it, we focused on the modules used for convolutional neural networks that have multiple branches and a merge layer. In the algorithm, the key ideas consisted of module detection ignoring long skip-connections, branch re-ordering for utilizing available memory maximally, assignment of MIFM and MOFM to share between modules, and branch processing. For Inception-V3 on Samsung’s NPU in Exynos, we showed the proposed algorithm achieved 97.59 % reduction in the amount of data to require off-chip access, and reduced the number of off-chip accesses by 1/50. Finally, we think the proposed algorithm can be a powerful solution to increase the efficiency of NPUs when processing various convolutional neural networks.

## References

- ARM-ML-processor. industry-leading performance and efficiency for inference at the edge. <https://developer.arm.com/products/processors/machine-learning/arm-ml-processor>.
- Courbariaux, M., Bengio, Y., and David, J.-P. Training deep neural networks with low precision multiplications. *arXiv preprint arXiv:1412.7024*, 2014.
- Courbariaux, M., Bengio, Y., and David, J.-P. Binaryconnect: Training deep neural networks with binary weights during propagations. In *Advances in Neural Information Processing Systems*, pp. 3123–3131, 2015.
- Gupta, S., Agrawal, A., Gopalakrishnan, K., and Narayanan, P. Deep learning with limited numerical precision. In *Proceedings of the 32nd International Conference on Machine Learning (ICML-15)*, pp. 1737–1746, 2015.
- Gysel, P., Motamedi, M., and Ghiasi, S. Hardware-oriented approximation of convolutional neural networks. *arXiv preprint arXiv:1604.03168*, 2016.
- Han, S., Mao, H., and Dally, W. J. Deep compression: Compressing deep neural networks with pruning, trained quantization and huffman coding. *arXiv preprint arXiv:1510.00149*, 2015.
- Han, S., Liu, X., Mao, H., Pu, J., Pedram, A., Horowitz, M. A., and Dally, W. J. Eie: efficient inference engine on compressed deep neural network. In *Computer Architecture (ISCA), 2016 ACM/IEEE 43rd Annual International Symposium on*, pp. 243–254. IEEE, 2016a.

- Han, S., Pool, J., Narang, S., Mao, H., Tang, S., Elsen, E., Catanzaro, B., Tran, J., and Dally, W. J. Dsd: Regularizing deep neural networks with dense-sparse-dense training flow. *arXiv preprint arXiv:1607.04381*, 2016b.
- He, K., Zhang, X., Ren, S., and Sun, J. Deep residual learning for image recognition. In *Proceedings of the IEEE conference on computer vision and pattern recognition*, pp. 770–778, 2016.
- Howard, A. G., Zhu, M., Chen, B., Kalenichenko, D., Wang, W., Weyand, T., Andreetto, M., and Adam, H. Mobilenets: Efficient convolutional neural networks for mobile vision applications. *arXiv preprint arXiv:1704.04861*, 2017.
- Hubara, I., Courbariaux, M., Soudry, D., El-Yaniv, R., and Bengio, Y. Quantized neural networks: Training neural networks with low precision weights and activations. *arXiv preprint arXiv:1609.07061*, 2016.
- Iandola, F. N., Han, S., Moskewicz, M. W., Ashraf, K., Dally, W. J., and Keutzer, K. Squeezenet: Alexnet-level accuracy with 50x fewer parameters and 0.5 mb model size. *arXiv preprint arXiv:1602.07360*, 2016.
- Judd, P., Albericio, J., Hetherington, T., Aamodt, T., Jerger, N. E., Urtasun, R., and Moshovos, A. Reduced-precision strategies for bounded memory in deep neural nets. *arXiv preprint arXiv:1511.05236*, 2015.
- Kim, D., Yim, H. Y., Ha, S., Lee, C., and Kang, I. Convolutional neural network quantization using generalized gamma distribution. *arXiv preprint arXiv:1810.13329*, 2018.
- Lin, D., Talathi, S., and Annapureddy, S. Fixed point quantization of deep convolutional networks. In *International Conference on Machine Learning*, pp. 2849–2858, 2016.
- Lin, M., Chen, Q., and Yan, S. Network in network. *arXiv preprint arXiv:1312.4400*, 2013.
- Long, J., Shelhamer, E., and Darrell, T. Fully convolutional networks for semantic segmentation. In *Proceedings of the IEEE Conference on Computer Vision and Pattern Recognition*, pp. 3431–3440, 2015.
- Ma, N., Zhang, X., Zheng, H.-T., and Sun, J. Shufflenet v2: Practical guidelines for efficient cnn architecture design. *arXiv preprint arXiv:1807.11164*, 2018.
- Ren, S., He, K., Girshick, R., and Sun, J. Faster r-cnn: Towards real-time object detection with region proposal networks. In *Advances in neural information processing systems*, pp. 91–99, 2015.
- Sandler, M., Howard, A., Zhu, M., Zhmoginov, A., and Chen, L.-C. Mobilenetv2: Inverted residuals and linear bottlenecks. In *Proceedings of the IEEE Conference on Computer Vision and Pattern Recognition*, pp. 4510–4520, 2018.
- Song, J., Cho, Y., Park, J.-S., Jang, J.-W., Lee, S., Song, J.-H., Lee, J.-G., and Kang, I. An 11.5tops/w 1024-mac butterfly structure dual-core sparsity-aware neural processing unit in 8nm flagship mobile soc. In *accepted for 2019 IEEE International Solid-State Circuits Conference (ISSCC)*.
- Szegedy, C., Liu, W., Jia, Y., Sermanet, P., Reed, S., Anguelov, D., Erhan, D., Vanhoucke, V., and Rabinovich, A. Going deeper with convolutions. In *Proceedings of the IEEE conference on computer vision and pattern recognition*, pp. 1–9, 2015.
- Szegedy, C., Vanhoucke, V., Ioffe, S., Shlens, J., and Wojna, Z. Rethinking the inception architecture for computer vision. In *Proceedings of the IEEE conference on computer vision and pattern recognition*, pp. 2818–2826, 2016.
- Tan, M., Chen, B., Pang, R., Vasudevan, V., and Le, Q. V. Mnasnet: Platform-aware neural architecture search for mobile. *arXiv preprint arXiv:1807.11626*, 2018.
- Zhang, S., Du, Z., Zhang, L., Lan, H., Liu, S., Li, L., Guo, Q., Chen, T., and Chen, Y. Cambricon-x: An accelerator for sparse neural networks. In *The 49th Annual IEEE/ACM International Symposium on Microarchitecture*, pp. 20. IEEE Press, 2016.